ELSEVIER

Polymer 41 (2000) 1167–1174

polymer

^{2}H NMR spin relaxation study of the molecular dynamics in poly(oxy-1,4-phenyleneoxy-1,4-phenylenecarbonyl-1,4-phenylene) (PEEK)

N.J. Clayden

School of Chemical Sciences, University of East Anglia, Norwich NR4 7TJ, UK

Received 8 January 1999; received in revised form 24 February 1999; accepted 18 March 1999

Abstract

Poly(oxy-1,4-phenyleneoxy-1,4-phenylenecarbonyl-1,4-phenylene) (PEEK) selectively ^{2}H labelled in the ether–keto rings has been studied by ^{2}H NMR T_1 relaxation time measurements. Partially relaxed ^{2}H NMR lineshapes at 360 K indicate the predominant dynamic process as a phenyl ring π flip. Computer simulations based on the model of a delta function for a rigid, crystalline phase and a log–normal distribution of phenyl ring flip rates for the amorphous phase, show that fits to a combination of a simple and stretched exponential are possible. However, accurate fits to the experimental ^{2}H saturation recovery curve based on exponential and stretched exponential functions could not be obtained over the full temperature range of 260–421 K. Constraining the fit to the trends seen in the computer simulations, allowed fits with only slightly increased errors suggesting that experimental error combined with the flexibility of the stretched exponential leads to the poor fits. The acquisition of improved experimental data is severely hampered by the long crystalline phase T_1. An estimate of the fast flipping fraction was made on the basis of the intensity after 100 ms recovery in the ^{2}H saturation recovery curve. From the increase in the fast flipping fraction with temperature, an energy of free volume formation of 10 ± 2 kJ mol^{-1} can be estimated. Evidence was found for fraction of the rings in the amorphous phase not undergoing π flips at the T_g.

Keywords: NMR; Poly(oxy-1,4-phenyleneoxy-1,4-phenylenecarbonyl-1,4-phenylene); Relaxation

1. Introduction

Poly(oxy-1,4-phenyleneoxy-1,4-phenylenecarbonyl-1,4-phenylene) (**I**) more commonly known as PEEK [1], is a tough semi-crystalline polymer with a crystalline melting point in the region of 335°C and a glass transition temperature, T_g, of about 145°C.

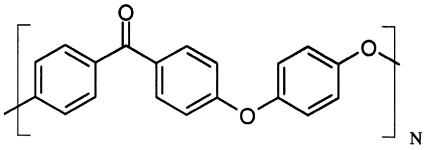

These thermal properties coupled with the high maximum in-service temperature and an excellent chemical resistance has led to its development as a high-quality engineering thermoplastic. In particular, sophisticated polymer composites such as APC2 [2] can be manufactured by fabrication with long carbon fibres. One attraction of PEEK as an engineering plastic is the maintenance of good mechanical properties over a wide temperature range. An important element in understanding the mechanical properties is a proper characterisation of the microscopic polymer chain dynamics, although it must be said that the precise manner in which the dynamic processes couple with the mechanical energy is largely unclear. To this end, the molecular motions in PEEK have been studied by a number of methods including dynamic mechanical spectroscopy [3,4], dielectric spectroscopy [5] and solid state NMR spectroscopy [6–9]. In addition, theoretical calculations have sought to identify the molecular constraints on the types of motion and hence the possible active modes [10]. CNDO calculations suggest that whereas the ether–ether ring is capable of π flips with an activation energy of 15.9 kJ mol^{-1}, the ether–keto rings are not. In contrast, the CPMAS ^{13}C NMR study by Poliks and Schaefer [6] demonstrated that at room temperature although most of the phenylene rings are immobile, at most 10–20% undergoing π flips, the ether–ether rings were somewhat more constrained than the ether–keto rings. In any event, a substantial fraction of the rings in the amorphous phase must be immobile. This is consistent with the idea of a rigid amorphous fraction in poorly crystallised PEEK as proposed by Wunderlich and co-workers on

0032-3861/00/$ - see front matter
PII: S0032-3861(99)00252-9

the basis of differential scanning calorimetry [11]. Although a precise comparison is not possible because of the differing thermal histories of the PEEK samples studied, the NMR results do indicate a far higher level of rigid amorphous polymer. ^{1}H spin–lattice relaxation time measurements under multiple pulse irradiation, $T_{1\times z}$, also suggest a three phase model is required to describe semi-crystalline PEEK [12]. Rather than a two exponential decay being seen for the magnetisation, three exponentials were required to fit the decay. Typical fractions, with relaxation times in brackets, for an amorphous PEEK annealed at 340°C for 4 h are: crystalline 0.31 (353.5 ms), intermediate 0.21 (21.1 ms) and amorphous 0.48 (3.2 ms). This highlights the difficulty with using the concept of a rigid amorphous fraction, since the fraction determined depends on the particular motion or motions being considered. In the case of the ^{13}C NMR results, rigid is identified as those rings not undergoing π flips. On the other hand, in the $T_{1\times z}$ measurements, the mechanism must be different, perhaps a torsional oscillation, otherwise the ^{13}C and ^{1}H approaches would yield contradictory results, with 48% of the ^{1}H nuclear spins undergoing some motion capable of causing relaxation, while only 10–20% of the ^{13}C nuclear spins relax at the same time. A further weakness of the idea of a rigid amorphous fraction is that, it ignores the widespread evidence from ^{2}H NMR studies of polymer dynamics, which show that dynamic processes are best described by distributions of correlation times [13]. The principal aim of the current work is to demonstrate whether or not a fraction of ether–keto rings in amorphous PEEK polymer remains rigid, that is not capable of π flips at or close to its T_g with the use of ^{2}H NMR spectroscopy on a PEEK selectively deuterated in the ether–keto rings, PEEK-d_8. A secondary aim is to characterise the fraction of aromatic rings in the fast motion limit, to see whether intermolecular constraints differ from the glassy phase of other polymers in terms of the average energy of hole formation [14,15]. As part of these aims, it is necessary to consider the accuracy of the data analysis based on non-linear least squares fitting to exponential and stretched exponential functions. In particular, the conditions under which the ^{2}H magnetisation can be analysed in terms of rigid and mobile fractions.

The results described are based on ^{2}H spin–lattice, T_1, relaxation times. A thorough knowledge of the spin–lattice relaxation time characteristics are essential, before any attempt can be made to partition elements of the lineshape into contributions from rigid and mobile fractions. Indeed, there is little sense in sophisticated modelling of the lineshape until the spin–lattice relaxation behaviour is characterised, particularly since the partially relaxed NMR spectrum often used to represent purely amorphous or mobile components depend on a recovery time after a saturating comb of pulses [16]. Evidence for ring flipping in PEEK can be seen in the partially relaxed ^{2}H NMR spectra at 363 K, where in order to resolve the separate effects of the ether–ether and ether–keto rings, selective deuteriation can be carried out on the ether–keto or ether–ether rings [9].

2. Experimental

2.1. Polymer

PEEK-d_8, corresponding to PEEK deuterated in the ether–keto rings was prepared using standard procedures [17], with the exception that d_8-difluorobenzophenone was used. The resulting polymer has a molecular weight distribution by GPC closely similar to the commercial grade PEEK 150G.

2.2. NMR measurements

^{2}H NMR measurements were made on a Bruker MSL200 NMR spectrometer operating at 30.7 MHz. A saturation recovery pulse sequence was used to measure the ^{2}H T_1 with a saturating comb of 10 π/2 pulses separated by 20 μs. The ^{2}H π/2 pulse was 3.3 μs and the rf pulses and amplitudes were optimised prior to data acquisition using a multiple pulse tune-up procedure. Four hundred transients were collected with a dwell time of 0.4 μs using a quadrupole-echo pulse sequence with an interpulse spacing of 40 μs. The recovery time was chosen in the range 10 μs to 300 s with 40 data points to represent the full saturation recovery curve. Data analysis was carried out using a non-linear least squares fitting algorithm based on the Levenberg–Marquardt method [18]. The functional form of the recovery was assumed to be either multi-exponential, stretched exponential or a combination of an exponential and stretched exponential. The noise level for the χ^2 significance test was based on the experimental signal-to-noise ratio seen in the longest recovery time NMR free induction decay.

2.3. Computer simulations

Computer simulations were carried out to assess the value of different fitting functions for describing the magnetisation recovery observed after initial presaturation in the PEEK samples, and thereby investigate the validity of partitioning the decay into contributions from rigid and mobile rings. The calculations took into account: the distribution of T_1 with correlation time, τ; the effect of echo reduction on the intensity of the quadrupole echo [19,20] and the orientation dependence of T_1 [21].

All simulations were based on the typical recovery times used experimentally, which were chosen to encompass the broad range of spin–lattice relaxation times expected in a polymeric system. The definition of the longer recovery times, in terms of the number of points and time interval between them, is less than satisfactory but is severely constrained by the data acquisition times. Towards the end of the saturation recovery curve, experimental points took

an excess of 1 day each to collect. Calculations were carried out assuming a log–normal distribution for the correlation times defined by a mean flip rate, Ω_m, and a variance, σ^2. The width of the distribution was taken as $\ln \Omega_m \pm \sigma$. For the majority of the simulated data sets, 41 elements were used to represent the distribution, extending over $\pm 2\sigma$. A few data sets were based on 101 and 201 elements to check the adequacy of the more restrictive model. No significant differences were seen for the data sets based on the larger number of elements. The model chosen to represent the polymer dynamics, and hence the ^{2}H spin–lattice relaxation mechanism was restricted π° flips. Intermediate exchange effects and the consequent attenuation of the quadrupole echo for flip rates between $10^{-7}\,\mathrm{s} < \tau < 10^{-4}\,\mathrm{s}$ was taken into account by calculating the free induction decay using the exchange matrix formalism [19].

Two types of fit were examined. First, multi-exponential fits and second a stretched exponential. Stretched exponentials, as represented by Eq. (1),

$$M(t) = M0(1 - \exp[-(t/\Xi)\beta]) \tag{1}$$

also known as a Kohlrausch–Willians–Watts function can be thought of as representing a superposition of exponential contributions and thus describing the likely physical picture of some distribution in T_1 determined by the distribution of ring flip rates. The average T_1 for the stretched exponential, $\langle T_1 \rangle$ can be defined through Eq. (2) [22,23]

$$\langle T_1 \rangle = \Xi/\beta\Gamma(\beta^{-1}). \tag{2}$$

Spin diffusion, which can lead to averaging of multi-site T_1 to a single value, is unlikely to be important except at very long T_1 values owing to the small dipolar coupling. Indeed, based on the lamellar thickness of 5 nm representative of virgin PEEK, we can estimate that a T_1 of 100 s would be possible before appreciable averaging by spin-diffusion takes place. However, to represent some spin-diffusional limit, a maximum T_1 of 50 s was used in the simulated data sets. Noise from a gaussian distribution of mean zero and standard deviation σ_n was added to each data point. Typically a value of 0.02 was chosen for σ_n with respect to the normalised intensity of 1.0, which represents a realistic experimental signal-to-noise ratio, achievable when recovery times of the order of 300 s have to be used. Calculations were carried out for two cases: (i) a single log–normal distribution representing both mobile and rigid polymer; and (ii) two distributions (one, a delta function, corresponding to the rigid fraction of the polymer $\phi_R = 0.3$ and the second a log–normal distribution for the mobile polymer, $\phi_M = 0.7$). A value of $\phi_R = 0.3$ was chosen for the rigid fraction as this represents a typical crystallinity seen for PEEK.

3. Results and discussion

3.1. Computer simulations

The treatment of broad distributions has led to the idea of populations of rings undergoing fast and slow flips. Often this choice is made on quite arbitrary grounds, and yet in the present case there is a need for an accurate assessment of the fast and slow flipping populations, if we are to say whether there is a rigid amorphous fraction. At its simplest, the distribution of rates for the ring flip in semi-crystalline PEEK must be bimodal, with a crystalline rigid component and an amorphous mobile component. The mean flip rate and variances are unknown as also is the nature of the two distributions, though there are strong grounds for adopting a log–normal distribution. These distributions will overlap, especially at low temperatures. We can interpret the rigid amorphous fraction in one of the two ways. First, it can represent another discrete distribution which may or may not change with temperature. Second, it may merely represent the slow flip rate end of the distribution of the amorphous polymer dynamics. Simulations of the spin–lattice relaxation characteristics are essential because of the concern about the extent to which the ^{2}H T_1 data can be analysed in terms of a rigid and mobile fractions, particularly when we are dealing with distributions of correlation times.

3.1.1. Single distribution

As expected, a single exponential function cannot satisfactory describe a ^{2}H magnetisation recovery curve arising from a polymer containing a distribution of ring flipping frequencies, except in the limit of a narrow distribution in flipping rates. Thus fitting errors are in excess of 4% even when the standard deviation of the flip rate distribution is just 1.4. Only when σ is about 0.8° the errors then fall below the 2% required for a statistically acceptable fit. Note, that typical experimental distribution widths for amorphous polymers derived from ^{2}H lineshape analyses, can be rather broad at 4.0 decades or more [24,25]. A log–normal distribution of variance σ^2 will have a width of $2\sigma \log e$ decades. Hard and fast rules about the magnitude of the fitting errors are, however, difficult to give, because the width of the distribution giving an acceptable fit also depends on the mean flip frequency. This is illustrated in Fig. 1 where the χ^2 seen in the fit is plotted as a function of Ω_m and σ. In general, the broader the ring flipping rate distribution, the lower the mean flipping rate should be for χ^2 to have a low value. Stretched exponentials will give an acceptable fit over a wider range of distribution widths, up to $\sigma \sim 2.6$. Overall, the values for χ^2 are an order of magnitude lower than for the simple exponential. But even so, as demonstrated in Fig. 2, larger errors than those strictly acceptable will be seen, when Ω_m is the region of intermediate exchange, 10^4–10^5 Hz. Characteristically, as σ increases β decreases, as shown in Fig. 3, demonstrating that the

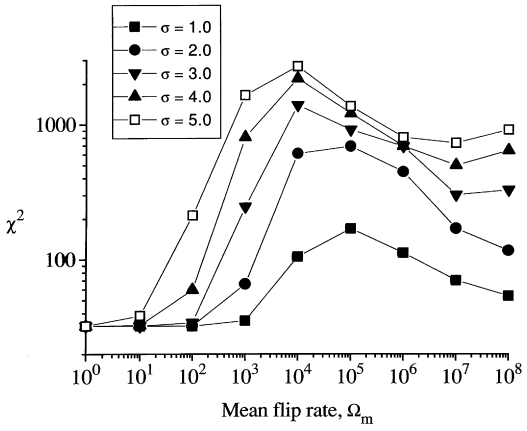

Fig. 1. Plot of χ^2 from a single exponential non-linear least squares fit to a computer simulated ^{2}H saturation recovery curve based on a single log–normal mobile distribution of phenyl ring π flips, with a mean flip rate Ω_m and variance σ^2. The expected χ^2 is 38.0, given two constraints, for which the goodness-of-fit Q is 0.5.

degree of non-exponential behaviour increases as the distribution becomes broader. This conclusion is in line with earlier work by Kulik and Prins [22], as well as Jeffrey et al. [24]. Similarly, increasingly broader distributions show a smaller value for Ξ, assuming that the correlation time for the ring flip lies on the slow motion side of the T_1 minimum. Finally, as the distribution is pushed across the T_1 minimum, Ξ begins to increase again. But it is important to note that when σ is in excess of 4.0, the fitting error even for the stretched exponential rises to about 4%, far exceeding the experimental noise. Consequently, a stretched exponential cannot be considered to give an adequate description of a broad distribution of flip rates, for example, when the distribution has a width of 3.5 decades.

The results of the stretched exponential fits to simulated log–normal distributions also calls into question the validity of the transformation of the distribution of T_1,($\rho(T_1)$ into a

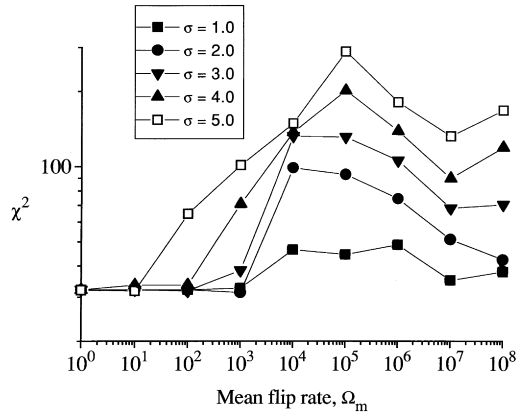

Fig. 2. Plot of χ^2 from a stretched exponential non-linear least squares fit to a computer simulated ^{2}H saturation recovery curve based on a single log–normal mobile distribution of phenyl ring π flips, with a mean flip rate Ω_m and variance σ^2. With three constraints, the expected χ^2 is 37.0, for which the goodness-of-fit Q is 0.5.

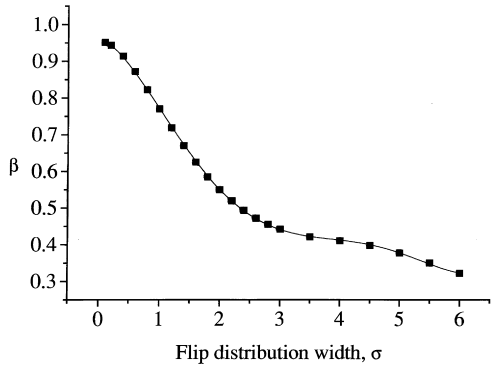

Fig. 3. Variation in the degree of non-exponential character (β) with the standard deviation of the distribution for the phenyl group π flips (σ). The solid line is shown to aid the eye and does not represent a fit to the data.

distribution of correlation times, $\rho_{T1}(\tau)$ presented by Kuliks and Prins [22]. In the case of polystyrene-d_3, they invert data with $\langle T_1\rangle \sim 1$ s and $\beta \sim 0.6$ to give a skewed distribution lacking long correlation times, yet a log–normal distribution of correlation times will give $\Xi = 0.63$ s and $\beta = 0.6682$ implying $\langle T_1\rangle = 0.83$ s, when $\tau_m = 0.37$ MHz and $\sigma = 1.54$. Removing the restriction of T_1 which might be thought to implicitly skew the distribution, has no influence on this conclusion, since $\Xi = 0.67$ s and $\beta = 0.6539$ when T_1 points out to a recovery time of 5000 s are included. Clearly, particular values of $\langle T_1\rangle$ and β, representative of Kulik and Prins data, can be obtained from a log–normal distribution showing either that the transformation is flawed or at least capable of yielding a number of correlation time distributions. This suggests that there is little value in trying to invert the T_1 data to get a correlation time distribution and hence partition the aromatic ring into fast and slow flipping fractions by this means.

Two exponential fits to the magnetisation recovery curve are almost as good as the stretched exponential ones, but the derived fractions for the short and long time constants components are essentially worthless, as they represent changing criteria for what constitutes a fast motion. For example, a two exponential fit of a log–normal distribution with $\sigma = 2.0$ gives an amorphous fraction of 0.37. Now calculating the cut-off frequency, Ω corresponding to this fraction and taking the amorphous component as the upper tail of the log–normal distribution, we find from the log–normal variate $x = (\ln \Omega - \ln \Omega_0)/\sigma$ that Ω is 0.74 MHz. On the other hand, when $\sigma = 3.0$, the amorphous fraction is found to be 0.57 giving the cut-off frequency for the upper tail as 0.2 MHz. With the previous definition for the cut-off frequency A would be only 0.41, a substantial difference in the amorphous fraction. Consequently, two exponential fits to a single distribution of T_1 values for ^{2}H relaxation in this type of system are meaningless in terms of defining a rigid and mobile fraction.

3.1.2. Two distributions

Two models were considered with the aim of testing how well a rigid fraction and a mobile one could be resolved;(i) a

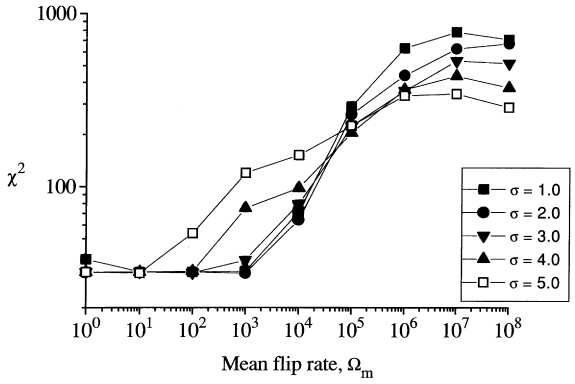

Fig. 4. Plot of χ^2 from a stretched exponential non-linear least squares fit to a computer simulated ^{2}H saturation recovery curve based on a rigid fraction, $\phi_R = 0.3$, and a mobile fraction $\phi_M = 0.7$, described by a log–normal distribution of phenyl ring π flips with a mean flip rate Ω_m and variance σ^2. The expected χ^2 is 37.0, for which the goodness-of-fit Q is 0.5.

stretched exponential and (ii) a stretched exponential with an exponential.

3.1.2.1. Stretched exponential A single stretched exponential only gives acceptable fits to the two distribution model when the mean flip rate for the mobile distribution is small, less than 10^4 Hz., as would be seen at low temperature, see Fig. 4. The reason for this being that at low flip rates, the mobile and rigid distributions overlap to such an extent they are effectively coincident. χ^2 tends to increase more rapidly when the log–normal distribution is narrow reflecting a greater divergence from the idea of a single distribution representing the phenyl ring π flips. These results clearly demonstrate that the low temperature ^{2}H NMR saturation recovery curve can be expected to fit to a single stretched exponential.

3.1.2.2. Stretched exponential and exponential Acceptable fits with <2% error were seen for the stretched exponential and exponential model over a wide range of mean flip rates

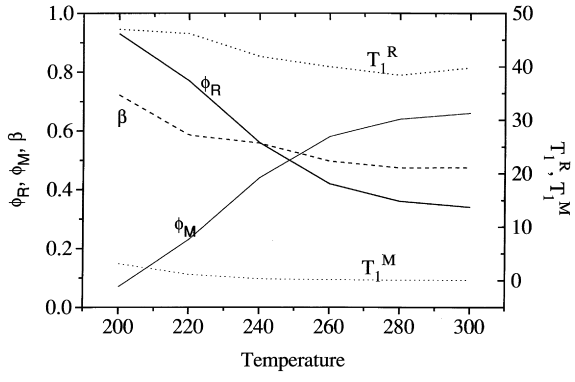

Fig. 5. Variation in the fitted parameters for an exponential and stretched exponential fit to a two distribution model of the phenyl ring flip rate. Mobile rings are represented by a log–normal distribution and rigid rings by a delta function. The mobile fraction is 0.3 and the limiting rigid ring T_1 is 50 s.

$\Omega_m = 1–10^8$ Hz and widths for the distribution, $\sigma = 1.0–5.0$. The errors exceed 2% only for intermediate mean flip rates, but in no case are greater than 2.6%. In practice, increasing temperature will tend to narrow the mobile distribution as well as shifting it to faster flip rates thereby minimising the possibility that the combined single exponential and stretched exponential will give larger errors. This was modelled by assuming an activation energy of 30 kJ mol^{-1} for the mean flip rate, and allowing the width to vary linearly with temperature in line, with upper and lower values seen for polystyrene-d_3 [24]. The effect on the fitting parameters is shown in Fig. 5. In all cases, the fit was statistically acceptable. At low temperature, the mobile distribution overlaps the rigid one and tends towards the limiting T_1. Thus, the fit is determined by simply an exponential with a small mobile component. As the temperature increases, the rigid fraction steadily decreases towards its limiting value $\phi_R = 0.3$ with the mobile distribution shifting to shorter correlation times. The shift ensures that it can be treated as a discrete distribution with the same results as that of a single distribution. This can be seen by β tending towards 0.475, consistent with a distribution of a standard deviation 2.6. Until very high temperatures, the long correlation time tail of the mobile fraction is incorporated into the rigid fraction, suggesting that it might prove almost impossible to distinguish between a true rigid amorphous fraction and simply a tail to the mobile amorphous distribution. All the fits to the simulated data sets, based on a rigid and mobile fraction with realistic parameters followed readily understandable trends, with fitting errors of less than 2.5%, demonstrating that analysis of this type of physical model is possible using the experimental ^{2}H spin–lattice relaxation saturation recovery results. Additional broadening of the rigid component will not affect the conclusion providing the distribution remains quite narrow, and is thus well represented by a simple single exponential. Some problems were, however, encountered when fitting to a simulated saturation recovery curve at low flip rate end, since the single exponential is sufficient to fit the data leading to a trade-off between the two functions resulting in physically unrealistic values for one or the other of the functions.

3.2. ^{2}H spin–lattice relaxation time measurements

All the experimental ^{2}H saturation recovery magnetisation curves were observed to be non-exponential, regardless of temperature, an example is shown in Fig. 6. Such behaviour is consistent with a distribution of flip rates for the dynamic process leading to ^{2}H relaxation. Despite the earlier computer simulations which suggested a single exponential and stretched exponential fit, would be adequate to represent the experimental data, severe problems were experienced analysing the low temperature data. In particular, the derived parameters showed little systematic trend with temperature. This is consistent with the interactions noted above between the exponential and stretched

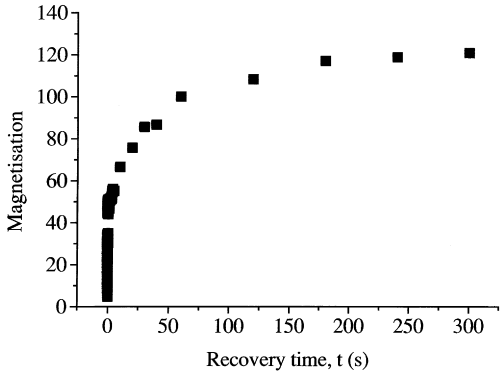

Fig. 6. ^{2}H NMR saturation recovery curve (30.7 MHz) for PEEK-d_8 at a temperature of 391 K.

exponentials when fitting low flip rate data. In contrast, at higher temperatures when the mobile and rigid polymer dynamics became well separated, acceptable fits could be obtained. Indeed, at lower temperatures, it was found to be preferable to use only a stretched exponential, even so the flexibility of the stretched exponential combined with the experimental error meant that no sensible trends could be derived as shown in Table 1. Partial confirmation that the difficulties experienced in the fitting were caused by these factors is provided by the results of constrained fits, where the value of Ξ was fixed for a given temperature to give a trend of decreasing $\langle T_1 \rangle$ with temperature for the mobile distribution. χ^2 for these constrained fits were only slightly in excess of those expected, and still gave a reasonable goodness-of-fit value Q of 0.01. The initial trend observed in terms of decreasing β and Ξ is consistent with the picture of a broad distribution being created by the mean flipping frequency of the mobile fraction moving to higher frequency, while the flipping frequency of the rigid component remaining essentially constant. A further reason for the difficulty in fitting the experimental saturation recovery curve is that, the curve is not sufficiently well defined at the longer recovery times. Some support for this is provided by the fits found in the ^{2}H data up to 1 s recovery time, where the stretched exponentials gave results consistent with the earlier computer simulations. Given that the ^{2}H T_1 for the rigid component (crystalline or amorphous) is largely temperature independent at ca. 45 s, we would

Table 1
Stretched exponential fits to the PEEK-d_8 saturation recovery curve. In the constrained fits, the value of Ξ was fixed at the value shown in the table

T (K)	Ξ (s)	Ξ^{con} (s)	β	β^{con}
260	3.34		0.551	
260		14.3		0.444
280	12.2		0.415	
300	9.2		0.391	
320	111.21		0.280	
320		5.0		0.335

Table 2

	Mobile			Rigid	
	ϕ_M	Ξ (ms)	β	ϕ_R	T_1 (s)
391 (K)	0.41	44.4	0.4219	0.59	45.0
420 (K)	0.35	19.9	0.5188	0.65	32.6

expect it to contribute at most 4% to the ^{2}H NMR signal after 1 s. The recovery of the rigid fraction magnetisation should correspond to the exponential component, since the distribution of flipping rates will be narrow. In addition to the poor definition of the recovery over the last data points arising from the small number of points, there will also be errors from the scatter in the experimental intensities. Given an intrinsic rms noise of ca. 2% of the maximum signal intensity, fluctuations as large as $\pm 4\%$ are possible 5% of the time. With 40 data points, we can expect two data points to have errors as large as this. This is particularly important at the cross-over between the rigid and mobile parts of the saturation recovery curve. Errors here will decide whether the mobile contribution appears to continue to increase or reaches a plateau. Taking the example of data collected at 300 K, unconstrained single exponential and stretched exponential fits gave a rigid T_1 of 195 s, indicating that the long recovery time data points are poorly defined. When the rigid T_1 is constrained to be 45.3 s, we find $\phi_R = 0.52$; $T_1 = 45.3$ s; and $\phi_M = 0.48$; $\Xi = 1.034$ s; $\beta = 0.4558$.

Two further sets of data collected at 300 K and analysed only over the first 1 s of the recovery gave results in good agreement, as follows: (i) $\Xi = 1.32$ s; $\beta = 0.4194$; and (ii) $\Xi = 1.12$ s; $\beta = 0.4126$. It should be noted as we are only fitting the mobile contribution to the saturation recovery curve, we do not obtain $\phi_{M,R}$. If these results where obtained from a log–normal distribution, then the mean jump frequency would be $\Omega_m = 0.14$ MHz, with a standard deviation, $\sigma \sim 2.8$, which corresponds closely to the jump frequency causing the maximum reduction in the echo signal intensity by intermediate exchange. Despite the value of constraining the rigid T_1 for the 300 K data, no similar benefit was seen for the data collected at 328 and 348 K. Both sets of data gave very low values for β, $\sim$0.25 and large values for Ξ, implying much larger values for the average T_1, $\langle T_1 \rangle$, which seemingly followed no consistent trend. One might expect $\langle T_1 \rangle$ to decrease with temperature as the mobile distribution is shifted towards shorter correlation times. Although a full statistical analysis of the effect of noise has not been carried out, the difficulties experienced in analysing the saturation recovery curves do not appear to be attributable to a poor signal-to-noise in the data, because when noisy data was computer simulated: log–normal distribution, $\Omega_0 = 0.36$ MHz and $\sigma \sim 3.0$, with $\sigma_n = 10\%$ $\langle T_1 \rangle$ only increased from 0.3 to 1.0 s with β decreasing from 0.508 to 0.397.

In light of these difficulties, no attempt was made to

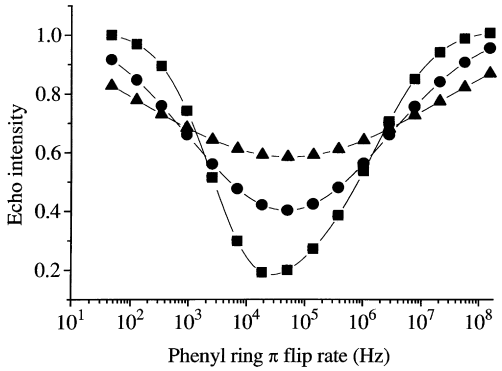

Fig. 7. Echo reduction factors in a ^{2}H quadrupole echo pulse sequence for a log–normal distribution of phenyl π flip rates based on a 50 μs echo delay as a function of the standard deviation of the distribution (■: $\sigma = 1.0$; ●:$\sigma = 3.0$; ▲: $\sigma = 5.0$).

characterise quantitatively the temperature variation in the ^{2}H saturation recovery curve in terms of mobile and rigid fractions. Instead, attention was turned to the specific question of whether a rigid amorphous fraction exists at or close to the T_g of PEEK. Here we can expect the analysis to be more straightforward, because the distribution associated with the mobile component will both be narrower than at lower temperatures and well shifted from the rigid one. A comparison of the mobile and rigid relaxation parameters at 391 K well below the T_g and at 420 K just above the T_g are shown in Table 2. Clearly in PEEK-d_8 above its T_g, the rigid fraction is in excess of the crystalline fraction demonstrating the presence of a rigid amorphous fraction. Moreover, this does not appear to correspond to the tail of an amorphous distribution, but represents a specific element in itself.

Over the temperature range studied 300–420 K, the intensity of the quadrupole echo signal showed a deviation less than 5% from the intensity expected on the basis of the Boltzmann factor. The question which arises is whether this is consistent with the nature of the distribution from the mobile component. Certainly, as the distribution describing the flipping frequency broadens the population of rings flipping with rates within the intermediate frequency range, will decrease and thus lessen the reduction in the echo intensity. Calculations indicate that when the log–normal distribution is defined by a standard deviation of 5.0, the signal reduction factor may vary from ~0.6 at the minimum to ~0.8 towards the fast motion limit, see Fig. 7. This would imply a deviation of only ±0.1 with respect to a mean intensity. Furthermore, if the mobile fraction distribution only constitutes 40% or so of the total intensity, it is perfectly plausible that the intensity of the observed signal will vary by less than 5%. Larger intensity variations are predicted if the distribution is narrower, consequently the observed intensity changes must imply that the distribution is indeed broad. Some support for this is provided by the ^{2}H NMR lineshapes, where essentially no change is seen in the lineshape as the quadrupole echo delay varied from 50 to 100 μs.

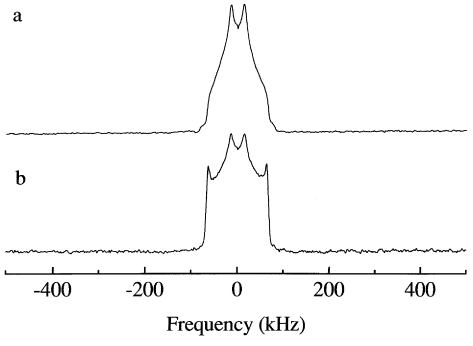

Fig. 8. ^{2}H quadrupole echo NMR spectra (30.7 MHz) of PEEK-d_8 at 391 K illustrating the presence of fast phenyl ring π flips: dwell time of 0.4 μs; and echo delay of 40 μs. (a) Partially relaxed spectrum acquired after a recovery time of 100 ms. (b) Fully relaxed spectrum acquired with a recovery time of 60 s.

3.3. Fast Flipping Fraction

Given the problems highlighted above in getting satisfactory fits to the complete saturation recovery curve for the ^{2}H magnetisation, a simpler approach was adopted towards estimating the fraction of aromatic rings undergoing fast π flips. Fast flips can be defined as having a correlation time $\tau < 10^{-7}$ s [14,16], implying a spin–lattice relaxation time, T_1 of the order of 55 ms, consequently the signal observed after a recovery time of 100 ms will closely approximate the fast flipping fraction. Clear evidence for the principal motion being π ring flips is provided by the ^{2}H NMR spectrum of PEEK-d_8 at 363 K, acquired in a partially relaxed NMR experiment using a recovery time of 100 ms (Fig. 8). No attempt was made to present a more sophisticated model for the ring dynamics in terms of additional ring motions. Commonly, the rate of ring flipping is discussed in terms of the local free volume, since it is reasonable to believe that an increase in the local free volume will facilitate the flipping process. Furthermore, since the free volume increases with temperature, we can expect the rings to be less constrained and thus more able to flip leading to an increase in the fraction of fast flippers. In essence, the broad distribution of aromatic ring flip rates present in the polymer is shifted to shorter correlation times. Qualitatively, this is observed with only 9% or so fast flipping at 260 K but 35% at 420 K, just above the T_g. More quantitatively, for a polymer glass the free volume fraction f can be expressed in terms of the absolute temperature, T, through the relationship

$$f = A \exp(-\varepsilon/\mathrm{RT}) \quad (3)$$

where A is approximately constant, ϵ is the mean thermodynamic energy required for the free volume formation, and R the gas constant. Assuming this relationship still holds for a semi-crystalline polymer and furthermore that the fraction of fast flipping aromatic rings is proportional to the fractional free volume, we can expect a linear relationship between ln f and the inverse temperature. It is not necessary

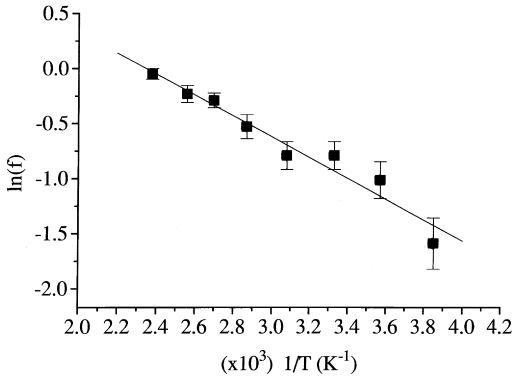

Fig. 9. Plot of the fast flipping fraction present in PEEK-d_8 as given by the intensity after 100 ms in the saturation recovery pulse sequence against the inverse temperature. The solid line is the linear least square regression fit.

to know the true amorphous factor *A*, since this will only introduce an error in the *y*-intercept. In the case of PEEK, the mean energy required to create sufficient free volume for a ring flip to take place derived from this relationship is 7.9 kJ mol^{-1} ($\ln A = 2.23$), with a correlation coefficient of -0.9762 (see Fig. 9). This energy derived for free volume formation is not only lower than that seen for glassy polymers where a value of the order of 15 kJ mol^{-1} is typical, but it is also lower than the value of 15.4 kJ mol^{-1} seen in broad line ^{1}H NMR studies [8]. However, it must be borne in mind that the ^{1}H NMR results represent an average activation energy for both the ether–ether and ether–keto rings and so do not necessarily conflict with the present ^{2}H NMR results based solely on the ether–keto rings. Although wide variations in the fast flipping fraction, and thus the derived energy of free volume formation are possible by altering the criterion for fast flipping, these still do not fully account for the discrepancy. For example, taking the intensity seen after a recovery time of 30 ms, the energy of free volume formation is 12 kJ mol^{-1} ($\ln A = 2.24$), correlation coefficient -0.965, while at further shorter recovery times and low temperatures, the signal-to-noise ratio limits the accuracy of the determination of the fast flipping fraction.

4. Conclusion

Computer simulations of ^{2}H saturation recovery decay curves representing a rigid component and broad mobile distribution suggest that analysis by a combination of a stretched and normal exponential will allow the two components to be separated. Multi-exponential fitting of similar data though expected to give statistically acceptable fits, does not give sensible fractions for the derived mobile and rigid components, because the frequency cut-off criterion defining the various phases is not a constant, but varies from data set to data set. Partially relaxed ^{2}H NMR spectra of PEEK-d_8 show that the ether–keto rings in PEEK are undergoing π flips, while the saturation recovery data indicates qualitatively that the proportion of fast flipping rings increases with temperature. Quantitative analysis of the saturation recovery curve over the full temperature range is hindered by the overlapping mobile and rigid distributions at intermediate temperatures, despite the evidence from the computer simulations that a fit should be possible. Inadequacies in the saturation recovery curve at long recovery times probably accounts for the difficulties, however, improving the data quality is severely limited by time constraints. At low temperatures, where the distribution associated with the higher temperature mobility overlaps the rigid phase, a single stretched exponential is adequate while at high temperatures where the mobile distribution is well separated, a stretched and normal exponential model can fit the data. Close to the *T*g, the fast flipping fraction is significantly less than the amorphous content based on the polymer crystallinity, indicating the presence of a rigid amorphous fraction. Moreover, the fraction is in excess of that expected from the long correlation time tail of the mobile fraction, suggesting a distinct rigid amorphous material. Analysis of the relaxation data based on the fast flipping fraction allows a energy of hole formation of 7.9 kJ mol^{-1} to be derived.

References

[1] Attwood TE, Dawson PC, Freeman JL, Hoy LRJ, Rose JB, Staniland PA. PEEK: poly(oxy-1,4 phenyleneoxy-1,4 phenylene carbonyl-1,4 phenylene). Polymer 1981;22:1096.
[2] Cogswell FN. Thermoplastic aromatic polymer composites. Oxford: Butterworth-Heinemann, 1992.
[3] Sasuga T, Hagiwara M. Polymer 1985;26:501.
[4] Sasuga T, Hagiwara M. Polymer 1986;27:821.
[5] Starkweather Jr. HW, Avakian P. Macromolecules 1989;22:4060.
[6] Poliks MD, Schaefer J. Macromolecules 1990;23:3426.
[7] Hay JN, Kemmish DJ. Polym Commun 1989;30:77.
[8] Clark JN, Jagannathan NR, Herring FG. Polymer 1988;29:341.
[9] Bunn A, Clayden N J, Newton AB. ACS Polymer Preprints 1988;29:8.
[10] Chen CL, Chang JL, Su AC. Macromolecules 1992;25:1941.
[11] Cheng SZD, Cao MY, Wunderlich B. Macromolecules 1986;19:1868.
[12] Clayden NJ. Bull Magn Reson 1993;15:70.
[13] Spiess HW. Coll Polym Sci 1983;261:193.
[14] Kaplan S, Conwell EM, Richter AF, MacDiarmid AG. Macromolecules 1989;22:1669.
[15] Chow TS. J Chem Phys 1983;79:4602.
[16] Jelinski LW. In: Komoroski RA, editor. High resolution NMR spectroscopy of synthetic polymers in bulk, Boca Raton, FL: VCH, 1986.
[17] Rose JB, Staniland PA. EP 1879;1982.
[18] Press WH, Flannery BP, Teukolsky SA, Vetterling WT. Numerical recipes: the art of scientific computing. Cambridge: Cambridge University Press, 1986.
[19] Mehring M. High resolution NMR in solids. 2nd ed. New York: Springer, 1983.
[20] Spiess HW, Sillescu. J Magn Reson 1981;42:381.
[21] Torchia DA, Szabo A. J Magn Reson 1982;49:107.
[22] Kulik AS, Prins KO. Polymer 1993;34:4642.
[23] Lindsey CP, Patterson GD. J Chem Phys 1980;73:3358.
[24] Montgomery CR, Bunce NJ, Jeffrey KR. J Phys Chem 1988;92:3635.
[25] Wehrle M, Hellman GP, Spiess HW. Coll Polym Sci 1987;265:815.